Measurements and Correlation of Two-Phase Pressure Drop Under Microgravity Conditions

I. Chen* and R. Downing
Sundstrand Corporation, Rockford, Illinois 61125
and
E. G. Keshock† and M. Al-Sharif‡
University of Tennessee, Knoxville, Tennessee 37916

Experimental data of two-phase pressure drop obtained in normal gravity and in nearly zero-gravity aboard a NASA-JSC KC-135 aircraft has been used to test the accuracy of a number of empirically based correlations and flow-regime dependent models. For the reduced-gravity data, the algorithms tested were: Lockhart and Martinelli, Troniewski and Ulbrich, Friedel, Chisholm B., Beattie and Whalley, an annular flow model using the Premoli void fraction correlation, and an annular flow model with an interfacial friction factor which was developed from the KC-135 reduced-gravity data. For the ground test results, the two annular models were replaced by stratified flow models, i.e., the Taitel-Dukler and Chisholm models. Based on this study, it was concluded that the pressure drops in reduced gravity and those of normal gravity are related to flow pattern models for each. The pressure drop predictions of the two annular flow models developed herein agreed well with the reduced-gravity data which were found to be significantly larger (by a factor of two or more) than the 1-*G* test data. The stratified models of Taitel-Dukler and Chisholm correlated best with the ground test data. For making predictions of two-phase pressure drop under microgravity conditions, flow-regime prediction and flow-regime dependent models appear essential.

Nomenclature

A = cross sectional
D = tube diameter
DP = pressure drop
dp/dz = pressure gradient
Fr = Froude number
f = friction coefficient
G = gravity
G_e = earth gravity
G_T = combined mass flux, liquid and vapor phases
h = depth of stratified liquid layer
j = superficial velocity
P = pressure
$\overline{P}$ = perimeter
Re = Reynolds number
S = interfacial width
$\overline{S}$ = slip ratio (gas velocity/liquid velocity)
u = velocity
We = Weber number
X = Martinelli parameter
x = quality
z = axial direction
y = stratified angle
α = void fraction
δ = film thickness
μ = absolute viscosity (dynamic)
ρ = density
σ = surface tension
τ = shear stress
Φ = two-phase friction multiplier

Subscripts
e = earth conditions
g = gas phase
go = gas flowing at total mass flux
i = interface
l = liquid phase
lo = liquid flowing at total mass flux
m = homogeneous mixture
w = wall
2Φ = two-phase mixture

Introduction

In comparison to those of small satellites, the increased heat loads anticipated for the NASA Space Station require more advanced thermal transport and temperature control techniques. A two-phase fluid loop provides significant thermal transport advantages in applications such as the Space Station. The required mass flows for a two-phase system are considerably less than those required to achieve the same isothermally using a pumped single-phase loop. The lower mass flow requirements result in the benefits of reduced pumping power, system size, and weight. Also, the comparatively larger heat transfer coefficients typical of phase change heat transfer processes can result in smaller heat exchangers with high heat flux capability. The design of a two-phase system for space applications would benefit greatly from realistic and accurate models for two-phase flow under reduced-gravity conditions. The understanding of two-phase flow has been greatly advanced in the past 40 years. However, very little empirical work and analytical modeling of two-phase flow have been done for conditions of reduced gravity.

The earliest studies of two-phase flow under reduced gravity conditions appear to have been those conducted at the NASA-Lewis Research Center in the early 1960s by Papell,[1] Evans,[2] Albers and Macosko,[3,4] and Block.[5] The study of Papell

Presented as Paper 89-0074 at the AIAA 27th Aerospace Sciences Meeting, Reno, NV, Jan. 9–12, 1989; received Feb. 23, 1989; revision received Oct. 26, 1990; accepted for publication Oct. 29, 1990.

*Staff Engineer, McDonald Douglas Space System Company, Houston, TX 77062.
†Professor and Chairman, Mechanical Engineering Department, Cleveland State University, Cleveland, OH 44115
‡Research Engineer, PAI Corporation, Oak Ridge, TN 37830.

focused upon instabilities developed during shutdown and startup of the subcooled boiling system, while the remaining NASA studies dealt primarily with flow visualization and pressure drop studies of air-water and condensing mercury flows. Also, in this same time period, Feldmanis[6] studied the performance of flow boiling and condensing loops under low-gravity conditions.

In the seventies, additional experimental studies of condensing two-phase flow were reported by Williams et al.,[7] Keshock et al.,[8] and Keshock[9] in which measurements of 1-G pressure drops were obtained, along with limited photographic observations, under the low-gravity conditions obtainable during KC-135 flight testing. Extensive studies by Hepner et al.[10] were conducted in 1975, in which flow-pattern observations and pressure drop measurements of an air-water flow were obtained, also in KC-135 tests. Although their test section length-to-diameter ratio was only 20, their pressure drop measurements were the best obtained to that point in what has been described by Dukler et al.[11] as a landmark study. Their measurements indicated higher values of pressure drop under conditions of low-gravity, compared with the results obtained for one-gravity conditions.

The most recent experimental studies of low-gravity liquid-vapor two-phase flows are those of Dukler et al.,[11] Hill and Downing,[12] and Hill et al.[13] The present paper is based upon the results obtained in the test program described in the latter two references.

More extensive reviews of both two-phase flow and heat transfer have recently been presented by Rezkallah[14] and Abdollahian.[15] A review article by Siegel[16] covers the reduced gravity experiments prior to 1967, while the review by Stark et al.[17] covers the pre-1974 literature. In brief, it may be said that while a very large number of studies have been conducted on 1-G, two-phase flow, only a very few studies have been conducted of low-gravity two-phase flows.

Thus, to increase the reduced-gravity data base and verify the current two-phase design philosophies, NASA-JSC contracted with Sundstrand to build a two-phase design thermal system test loop that could be both ground-tested and flown aboard the NASA KC-135 aircraft flying parabolic trajectories for evaluation under reduced-gravity conditions. This study, described by Hill, et al.,[12] demonstrated the performance of a two-phase thermal management system incorporating prototypical components. Details of the experimental test rig, the ground and flight test sequence, and the system response are presented by Hill, et al.[13] together with an overview of the observed flow regimes and the measured pressure drop data for the two-phase flow section. The companion paper[18] to this work focuses on the correlation of the observed flow patterns to a variety of flow regime maps.

To avoid excessive conservatism in either the plumbing or pumping design for the Space Station, accurate two-phase pressure drop models are needed. Currently available two-phase pressure drop models are empirically or semi-empirically derived from terrestrial test data. Because the microgravity two-phase pressure drop data base is severely limited, new correlations developed for space applications must be taken as preliminary. One such correlation, based upon the data obtained from the Sundstrand/University of Tennessee/NASA-JSC experiment, is included here. The proposed correlation is phenomenologically consistent with the test results, which showed a predominance of annular flow over a large range of thermodynamic quality. The interfacial friction factor used in the model is inferred from the reduced-gravity pressure drop data.

Until the time when the microgravity pressure drop models reach full maturity, the aerospace community must select and use the most appropriate ground-based correlations. Towards this effort, this paper screens the microgravity test data against nine popular models and assesses their validity to the new data. The degree of correlation indicates the conservatism needed in a space platform two-phase thermal bus design.

Experimental Apparatus and Results

The schematic for the pressure drop test section is shown in Fig. 1. Saturated two-phase Refrigerant-114 at various qualities flowed through a 0.623-in (1.58 cm) diameter adiabatic clear section, which included a 72-in long (1.83 m) straight section and a curved section with a 180 deg bend. The test section was instrumented with pressure transducers as shown in Fig. 1. The nominal accuracy of the differential pressure transducers was ± 345 Pa (± 0.05 psi), and the calibrated flow meters are accurate to $\pm 2\%$ of their nominal value.

Ground tests of the combined two-phase flow test section and thermal management system were first performed to develop a suitable basis of comparison for the low-gravity operational data. Tests were then performed aboard the NASA KC-135 aircraft on two separate days (4/16/87 and 4/17/87) to obtain reduced-gravity conditions during Keplerian flight trajectories. Fifty-four parabolas were flown, in sets of three. During each set, the same nominal flow quality and test conditions existed. From one set to another, the vapor quality, x, was varied over the range of 0.05 to 0.90. At the highest quality, the mass flux, G_T, was roughly 191 kg/m^2-s (39 lbm/ft^2-s), increasing to 230 kg/m^2-s (47 lbm/ft^2-s) at the lowest quality.

Within each parabola, the three axis G-fields could be held below about ± 0.05 earth gravity for roughly a 20-s period in the reduced-gravity test. The averaged test data for the reduced gravity conditions for 43 of the parabolas is presented in Table 1. Nine of the parabolas were judged to be outside the ± 0.05 G_e bounds for part of the reduced gravity period. A temporal average of the three-axis vectorial G-field sum is included in Table 1. For each parabola the pressure drop was the average of 7 or 8 values sampled during the 20-s low gravity period, i.e., once approximately every 2.5 s. Flow equilibrium conditions appeared to have been established very quickly after the pullout from 2-G conditions into the low-gravity period. Typically, a slug flow in the 2-G condition would change to a Taylor bubble type flow, for example, in less than 1 s. The ground test data taken on the straight section before and after the flights is shown in Table 2. Pressure drop data at the very low-quality flows must be accepted with caution because of the greater relative error in these measurements.

Flow Regime Observations

In two-phase liquid-vapor flows inside tubes, the pressure drop is intimately related to the flow pattern because different two-phase structures (interfacial configurations) yield different momentum and frictional characteristics. Many correlations of pressure drop have been proposed that are not flow-regime dependent, but such correlations are empirically based and must be considered valid only within the limited range of the data on which they are based. Accordingly, knowledge of the flow regime in any two-phase flow significantly improves the accuracy to be expected in predicting the pressure drop.

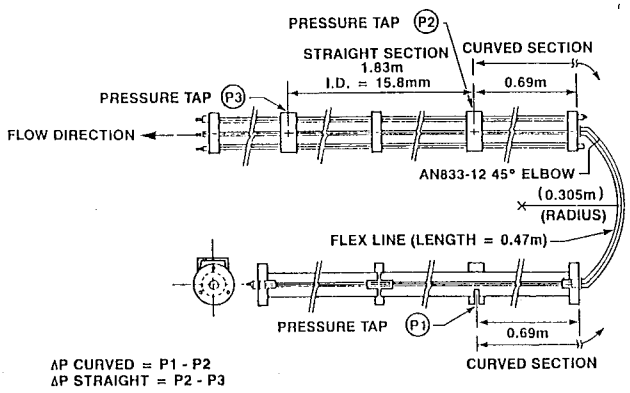

Fig. 1 Adiabatic two-phase pressure-drop test section.

Table 1 Straight section pressure drop measurements under reduced-gravity conditions

RUN	X Vapor quality	G_T LBM/s-ft²	G_T kg/m²-s	DP PSID	DP KPA	G/G_e	P PSIA	P MPA
1	0.147	45.881	224.48	0.046	0.320	0.006	92.757	0.6395
2	0.146	46.133	225.71	0.031	0.210	0.007	92.699	0.6391
3	0.146	46.009	225.11	0.047	0.320	0.013	92.699	0.6391
4	0.199	45.397	222.11	0.058	0.324	0.008	92.885	0.6402
5	0.199	45.434	222.29	0.056	0.386	0.006	92.752	0.6395
6	0.198	45.643	223.32	0.059	0.407	0.014	92.590	0.6384
7	0.278	44.518	217.81	0.087	0.600	0.002	93.055	0.6416
8	0.278	44.667	218.54	0.075	0.517	0.008	92.963	0.6409
9	0.277	44.750	218.95	0.074	0.510	0.006	92.983	0.6411
10	0.406	43.483	212.75	0.145	1.000	0.005	93.406	0.6440
11	0.407	43.276	211.74	0.145	1.000	0.004	93.210	0.6427
12	0.406	43.388	212.28	0.140	0.965	0.001	93.154	0.6423
13	0.623	41.713	204.09	0.193	1.331	0.016	93.982	0.6480
14	0.623	41.731	204.18	0.210	1.448	0.015	93.647	0.6457
15	0.622	41.728	204.16	0.196	1.351	0.015	93.698	0.6460
16	0.864	40.821	199.72	0.219	1.510	0.027	94.430	0.6511
17	0.862	40.823	199.73	0.221	1.524	0.025	94.387	0.6508
18	0.863	40.829	199.76	0.223	1.538	0.003	94.280	0.6500
19	0.052	46.948	229.70	0.009	0.062	0.003	91.549	0.6312
20	0.051	47.287	231.36	0.011	0.076	0.011	91.598	0.6315
21	0.892	39.683	194.16	0.265	1.827	0.008	95.470	0.6582
22	0.891	39.279	192.18	0.263	1.813	0.001	95.494	0.6584
23	0.897	39.022	190.92	0.243	1.675	0.023	95.673	0.6596
24	0.645	40.649	198.88	0.221	1.524	0.008	94.392	0.6508
25	0.645	40.574	198.52	0.227	1.565	0.011	94.404	0.6509
26	0.650	40.295	197.15	0.234	1.613	0.010	94.524	0.6517
27	0.540	41.365	202.39	0.180	1.241	0.014	93.982	0.6480
28	0.541	41.218	201.67	0.181	1.248	0.013	93.964	0.6478
29	0.538	41.290	202.02	0.188	1.296	0.010	93.753	0.6464
30	0.283	43.608	213.36	0.105	0.724	0.002	93.109	0.6420
31	0.283	43.683	213.73	0.117	0.807	0.016	92.938	0.6408
32	0.282	43.793	214.27	0.119	0.820	0.005	93.028	0.6414
33	0.197	44.741	218.90	0.077	0.531	0.006	92.690	0.6391
34	0.197	44.618	218.30	0.073	0.503	0.027	92.565	0.6382
35	0.197	44.732	218.86	0.061	0.421	0.000	92.469	0.6375
36	0.151	45.035	220.34	0.061	0.421	0.016	92.321	0.6365
37	0.150	45.437	222.31	0.053	0.365	0.018	92.192	0.6356
38	0.151	45.173	221.02	0.063	0.434	0.011	92.097	0.6350
39	0.093	46.681	228.40	0.029	0.200	0.000	91.851	0.6333
40	0.096	45.624	223.22	0.028	0.193	0.000	91.462	0.6306
41	0.414	42.673	208.79	0.156	1.076	0.010	92.297	0.6364
42	0.413	42.817	209.49	0.143	0.986	0.007	92.322	0.6365
43	0.405	43.527	212.96	0.141	0.972	0.010	92.601	0.6385

Table 2 Straight section pressure drop measurements under ground gravity conditions

RUN	X Vapor quality	G_T LBM/s-ft²	G_T kg/m²-s	PSID	DP	G/G_e	P PSIA	P MPA
1	0.162	62.119	303.93	0.035	0.241	1.000	95.150	0.6560
2	0.230	43.630	213.47	0.017	0.117	1.000	95.700	0.6598
3	0.896	40.126	196.32	0.118	0.814	1.000	97.460	0.6720
4	0.896	40.126	196.32	0.123	0.848	1.000	97.600	0.6729
5	0.659	40.126	196.32	0.106	0.731	1.000	97.270	0.6706
6	0.646	40.998	200.59	0.091	0.627	1.000	96.960	0.6685
7	0.645	40.999	200.60	0.081	0.558	1.000	96.880	0.6680
8	0.429	41.872	204.87	0.055	0.379	1.000	96.420	0.6649
9	0.428	41.977	205.38	0.048	0.331	1.000	96.250	0.6636
10	0.517	34.878	170.65	0.034	0.234	1.000	96.330	0.6642
11	0.099	46.622	228.11	0.010	0.069	1.000	95.430	0.6580
12	0.151	45.388	222.07	0.013	0.090	1.000	95.520	0.6586
13	0.140	58.300	285.24	0.032	0.221	1.000	43.500	0.2999
14	0.284	62.197	304.31	0.050	0.335	1.000	84.840	0.5849
15	0.153	43.630	213.47	0.009	0.062	1.000	95.500	0.6584
16	0.210	43.551	213.08	0.014	0.097	1.000	95.620	0.6593
17	0.896	40.126	196.32	0.111	0.765	1.000	97.350	0.6712
18	0.896	40.126	196.32	0.113	0.779	1.000	97.410	0.6716
19	0.920	40.126	196.32	0.120	0.827	1.000	97.490	0.6722
20	0.894	40.126	196.32	0.120	0.827	1.000	97.450	0.6719

Table 2 *(Continued)*

RUN	X Vapor quality	G_T LBM/s-ft²	G_T kg/m²-s	PSID	DP	G/G_e	P PSIA	P MPA
21	0.646	41.006	200.63	0.087	0.600	1.000	96.960	0.6685
22	0.645	40.992	200.22	0.082	0.565	1.000	96.870	0.6679
23	0.646	40.992	200.22	0.085	0.586	1.000	96.850	0.6677
24	0.428	41.963	205.31	0.051	0.352	1.000	96.360	0.6644
25	0.425	42.095	205.96	0.049	0.338	1.000	96.270	0.6637
26	0.426	42.226	206.60	0.047	0.324	1.000	96.250	0.6636
27	0.520	34.733	169.94	0.038	0.262	1.000	96.390	0.6646
28	0.714	25.286	123.72	0.028	0.193	1.000	96.560	0.6657
29	0.609	30.508	149.27	0.056	0.386	1.000	97.240	0.6704
30	0.408	44.207	216.29	0.059	0.407	1.000	96.330	0.6642
31	0.606	43.696	213.79	0.081	0.558	1.000	96.710	0.6668
32	0.756	34.878	170.65	0.064	0.441	1.000	96.740	0.6670
33	0.138	58.287	285.18	0.034	0.234	1.000	43.540	0.3002
34	0.196	60.295	295.00	0.039	0.269	1.000	63.480	0.4377
35	0.293	62.119	303.93	0.053	0.365	1.000	85.080	0.5867
36	0.278	62.867	307.59	0.050	0.335	1.000	95.260	0.6568
37	0.144	61.935	303.03	0.031	0.214	1.000	95.030	0.6552
38	0.167	53.668	262.58	0.018	0.124	1.000	95.370	0.6575
39	0.202	44.102	215.78	0.014	0.097	1.000	95.580	0.6590
40	0.157	43.722	213.92	0.012	0.083	1.000	95.540	0.6587
41	0.290	43.577	213.21	0.023	0.159	1.000	95.770	0.6603
42	0.288	43.512	212.89	0.026	0.179	1.000	95.870	0.6610
43	0.290	43.381	212.25	0.028	0.193	1.000	95.880	0.6611
44	0.290	43.407	212.38	0.028	0.193	1.000	95.910	0.6613
45	0.502	42.948	210.13	0.040	0.276	1.000	96.050	0.6622
46	0.532	42.685	208.84	0.054	0.372	1.000	96.380	0.6645
47	0.533	42.685	208.84	0.057	0.393	1.000	96.490	0.6653
48	0.539	42.226	206.60	0.064	0.441	1.000	96.580	0.6659
49	0.628	41.858	224.37	0.073	0.503	1.000	96.580	0.6659
50	0.634	41.858	204.80	0.078	0.538	1.000	96.710	0.6668
51	0.633	41.858	204.80	0.076	0.524	1.000	96.750	0.6671
52	0.645	41.097	201.07	0.082	0.565	1.000	96.780	0.6673
53	0.636	41.675	203.90	0.080	0.552	1.000	96.820	0.6675
54	0.860	40.992	200.56	0.104	0.717	1.000	97.190	0.6701
55	0.894	40.205	196.71	0.120	0.827	1.000	97.470	0.6720
56	0.897	40.113	196.26	0.124	0.855	1.000	97.500	0.6722
57	0.841	42.738	209.10	0.125	0.862	1.000	97.530	0.6724
58	0.823	43.617	213.40	0.134	0.924	1.000	97.580	0.6728
59	0.827	43.604	213.34	0.137	0.945	1.000	97.610	0.6730
60	0.389	46.162	225.86	0.066	0.455	1.000	96.380	0.6645
61	0.385	46.582	227.91	0.052	0.359	1.000	96.200	0.6633
62	0.380	47.488	232.34	0.041	0.283	1.000	98.500	0.6791
63	0.381	47.790	233.82	0.057	0.393	1.000	102.500	0.7067
64	0.388	46.359	226.82	0.070	0.483	1.000	96.600	0.6660
65	0.384	46.779	228.87	0.055	0.379	1.000	96.200	0.6633
66	0.387	46.504	227.53	0.050	0.345	1.000	96.140	0.6629
67	0.384	46.753	228.75	0.053	0.365	1.000	96.130	0.6628
68	0.376	46.963	229.78	0.060	0.414	1.000	88.570	0.6107
69	0.376	46.714	228.56	0.066	0.455	1.000	84.820	0.5848
70	0.186	47.895	234.34	0.031	0.214	1.000	80.690	0.5563
71	0.364	48.446	237.03	0.049	0.338	1.000	84.700	0.5840
72	0.367	48.446	237.03	0.047	0.324	1.000	89.930	0.6200
73	0.156	45.126	220.79	0.009	0.062	1.000	95.176	0.6562
74	0.209	44.798	219.18	0.015	0.103	1.000	95.286	0.6570
75	0.288	44.391	217.19	0.026	0.179	1.000	95.510	0.6585
76	0.420	43.892	214.75	0.044	0.303	1.000	95.870	0.6610
77	0.514	43.367	212.18	0.061	0.421	1.000	96.160	0.6630
78	0.627	42.501	207.94	0.079	0.545	1.000	96.420	0.6648
79	0.869	41.557	203.33	0.115	0.793	1.000	97.080	0.6693

Consequently, to more accurately develop a model for predicting pressure drop under microgravity conditions, direct observations of the nature of two-phase flow under the low-gravity conditions occurring during the KC-135 tests were made. The flow patterns were observed within the transparent test section illustrated in Fig. 1, using high-speed photography. The flow patterns observed are described in Table 3. The description encompasses flow over a range of qualities from 0.05 to 0.86, for both 1-G conditions (ground testing, horizontally oriented test section) and the reduced-g conditions during the KC-135 parabolic trajectories. A more extensive description of the observed flow patterns, together with comparisons of several flow regime maps, is presented by Chen et al.[18]

In brief, during low-G conditions, slug flow was observed over the quality range from 5 to 10%. The slug flow consisted

Table 3 Summary of observed flow patterns under reduced and ground gravity conditions

Nominal quality (%)	j_g (ft/s) m/s	j_l (ft/s) m/s	Flow characteristics
5	(0.85) 0.259	(0.54) 0.165	1-*G*: Stratified-wavy. 0-*G*: Taylor bubbles, coalescing into larger ones. Small bubbles entrained in liquid region in wake of Taylor bubbles.
10	(1.56) 0.475	(0.51) 0.155	1-*G*: Stratified-wavy. Small amplitude rollwaves, occasional change to a slug flow. 0-*G*: Very long Taylor bubbles, with many small bubbles in wake. Appears as annular flow, except in relatively small region between Taylor bubbles.
15	(2.34) 0.713	(0.47) 0.143	1-*G*: Stratified-wavy. Waves are of smaller amplitude. 0-*G*: Annular flow, thick annular film, some wavy undulations in film. Initially some evidence of noncontinuous annular pattern, i.e., vapor core interrupted by all liquid region.
20	(3.13) 0.954	(0.44) 0.134	1-*G*: Stratified-ripply interface, with roll waves (surges) spaced about 4 ft apart. 0-*G*: Classical annular flow pattern.
28	(4.30) 1.311	(0.39) 0.119	1-*G*: Stratified with roll waves ("surfing" waves) developed periodically. 0-*G*: Classical annular flow pattern. No evidence of disturbance waves (bands) specifically noted.
41	(6.07) 1.850	(0.31) 0.094	1-*G*: Stratified. Periodic roll waves (surges) 0-*G*: Annular flow.
54	(7.61) 2.320	(0.23) 0.070	1-*G*: Semi-annular flow, stratified layer, but with thin, finely rippled annular film around upper periphery of tube. 0-*G*: Annular flow with disturbance waves (bands) moving along interface.
62	(8.92) 2.719	(0.19) 0.0579	1-*G*: Semi-Annular flow. Same as at 50 percent. 0-*G*: Annular flow. Both small amplitude waves and larger disturbance waves in annular liquid film.
86	(11.98) 3.652	(0.069) 0.021	1-*G*: Annular flow with slightly thicker stratified layer. 0-*G*: Annular flow. Smaller amplitude ripples than at lower qualities, closely spaced, disturbance waves (bands) also moving along annular film.

of perfectly centered Taylor bubbles separated by predominantly liquid regions that included smaller, entrained spherical bubbles. It appeared that the smaller bubbles were primarily generated at the wake of the Taylor bubble. A transition to annular flow occurred between 10 and 15% quality, which then persisted up to the maximum nominal quality observed, 86%. Thus, annular flow existed over a quality range from roughly 15 to 90%. At very low quality (<5%) one might expect a dispersed bubbly flow pattern, while at the very highest quality, a dispersed mist flow could be reasonably anticipated. Neither of these extremes was within the scope of the test conditions, however.

Thus, under low-gravity conditions, after a brief interval of bubbly and slug flow, an annular flow pattern exists up to quality levels approaching 90%. A model for predicting pressure drop based on an annular flow pattern for qualities greater than about 10% would, therefore, appear to be quite reasonable.

The pressure drop tests showed that the measured pressure drop under reduced gravity are considerably higher than the equivalent 1-*g* data, as shown in Fig. 2. This basic difference apparently is related to the different flow patterns which occurred under the ground and microgravity conditions. For example, for qualities above 0.15, annular flow occurred in the reduced-gravity tests, while wavy-stratified and slug flows prevailed over the entire range of qualities in the ground test.

Two-Phase Pressure Drop Predictions

The pressure drop measured across the straight section in both the ground and flight tests were correlated to a number of two-phase pressure drop models. Because the test section was nearly adiabatic and the gravitational pressure drop component is negligible in both the reduced-gravity and ground horizontal tests, only the two-phase frictional pressure drop is considered for the correlations. For the reduced-gravity data, the algorithms of Lockhart-Martinelli,[19] Troniewski and Ulbrich,[20] Friedel,[21] Chisholm B.,[22] and Beattie and Whalley,[23] were tested. An annular flow model using the Premoli et al.[24] void fraction correlation was developed to compare with the high-quality reduced-gravity data.

To correlate the ground test results, the annular model was replaced by two stratified flow models, i.e., Taitel and Dukler[25] and Chisholm.[26] Generally, the Chisholm model is empirically based, and Taitel and Dukler's is based on physical modeling of the stratified flow pattern.

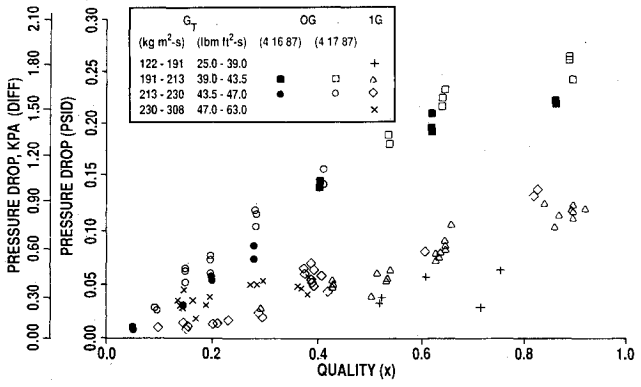

Fig. 2 Ground and reduced-gravity pressure drop data of R-114 vapor and liquid mixture.

The above methods of calculating frictional pressure gradient in two-phase flow are briefly summarized below.

Beattie and Whalley

In the Beattie-Whalley[23] algorithm, the two-phase flow is considered to be a homogeneous mixture, having an average density given by

$$\frac{1}{\rho_m} = \frac{x}{\rho_g} + \frac{1 - x}{\rho_l} \tag{1}$$

and an average viscosity given by

$$\mu_m = \mu_g \alpha_m + \mu_l(1 - \alpha_m)(1 + 2.5\alpha_m) \tag{2}$$

where α_m is the homogeneous void fraction given by

$$\alpha_m = \frac{\rho_l x}{\rho_l x + \rho_g(1 - x)} \tag{3}$$

The frictional pressure gradient is calculated using the Fanning equation for single-phase flow, but modified to use the homogeneous fluid properties. Thus

$$\left(\frac{dp}{dz}\right)_{2\Phi} = -\frac{2f_m G_T^2}{\rho_m D} \tag{4}$$

where the friction factor f_m is based on the homogeneous Reynolds number, $Re_m = G_T D/\mu_m$. The G_T is the two-phase mixture mass flux and D is the tube diameter.

Lockhart-Martinelli

The Lockhart-Martinelli method[19] is one of the oldest and most widely used techniques for calculating two-phase flow pressure drops. The two-phase pressure drop is a multiple of the single-phase pressure drop calculated assuming liquid alone flows in the tube at G_1, or the vapor phase in the tube at G_g. These multipliers, Φ_l^2 or Φ_g^2, are given by

$$\Phi_l^2 = \frac{(dp/dz)_{2\phi}}{(dp/dz)_l} \tag{5}$$

$$\Phi_g^2 = \frac{(dp/dz)_{2\phi}}{(dp/dz)_g} \tag{6}$$

and are related to the parameter X^2 given by

$$X^2 = \frac{(dp/dz)_l}{(dp/dz)_g} \tag{7}$$

The relationship of Φ_l^2 and Φ_g^2 to X^2 was originally presented in graphical form, but Chisholm[27] has approximated these relationships by the expressions:

$$\Phi_l^2 = 1 + C/X + 1/X^2 \tag{8}$$

$$\Phi_g^2 = 1 + CX + X^2 \tag{9}$$

Tabular constants for C are given by Chisholm, depending on whether the individual phases are laminar or turbulent flow.

Troniewski and Ulbrich

Troniewski and Ulbrich[20] proposed different expressions for describing the graphic relationship between Φ_l^2 and Φ_g^2 to X originally proposed by Lockhart and Martinelli. These expressions are as follows:

$$\Phi_g = \begin{cases} \exp\left|\sum_{m=0}^{5}[a_m(\ell n x)^m]\right|; & 0.01 < x < 100 \quad (10a) \\ \exp|a_6 \exp(a_7 \ell n x)]; & x \le 0.01 \quad (10b) \\ \Phi_l = \exp|a_8 \exp(a_9 \ell n x)|; & x \ge 100 \quad (11) \end{cases}$$

The two-phase frictional pressure gradient is obtained from

$$\left(\frac{dp}{dz}\right)_{2\Phi} \equiv \begin{cases} \left(\frac{dp}{dz}\right)_l \Phi_l^2; & x \ge 100 \quad (12a) \\ \left(\frac{dp}{dz}\right)_g \Phi_g^2; & x < 100 \quad (12b) \end{cases}$$

Constants for Eqs. (10) and (11) are given by Troniewski and Ulbrich.[20] Although this model is quite complex in form, when compared with other methods available in the literature for calculating the multipliers, Φ_l^2 and Φ_g^2, it was found to yield the smallest errors.[28]

Friedel

Friedel[21] proposed a method based on a bank of 25,000 two-phase pressure drop data points. He proposed a multiplier defined by

$$\Phi_{lo}^2 \equiv \frac{(dp/dz)_{2\Phi}}{(dp/dz)_{lo}} \tag{13}$$

where $(dp/dz)_{lo}$, is the single-phase pressure gradient calculated by assuming the total flow to be liquid flow at G_T^2. His correlation (for both horizontal and vertical upward flow) is given by

$$\Phi_{lo}^2 = E + 3.24FH/(Fr^{0.045}We^{0.035}) \tag{14}$$

where

$$E = (1 - x)^2 + x^2(\rho_l f_{go}/\rho_g f_{lo}) \qquad F = x^{0.78}(1 - x)^{0.24}$$

$$H = (\rho_l/\rho_g)^{0.19}(\mu_g/\mu_l)^{0.19}(1 - \mu_g/\mu_l)^{0.7}$$

$$Fr = G_T^2/(gD\rho_m^2) \qquad We = G_T^2 D/(\rho_m \sigma)$$

Although Friedel's correlation has been reported to work extremely well, Whalley[29] recommended its use be limited to $(\mu_l/\mu_g) < 1000$ as a result of recent evaluations against a proprietary data bank.

Chisholm

Chisholm's correlation[22] (for turbulent flow) can be summarized again in terms of a multiplier based on liquid alone flowing at the total flow rate

$$\Phi_{lo}^2 = 1 + (\Gamma^2 - 1)\left|Bx^{(2-m)/2}(1-x)^{(2-m)/2} + x^{(2-m)}\right| \tag{15}$$

where m = power on the friction factor-Re relationship used ($M = 0.025$ for the Blasius relationship), and

$$\Gamma^2 \equiv (dp/dz)_{fo}/(dp/dz)_{lo} \tag{16}$$

The parameter B is given by Chisholm. This method tends towards overprediction at low-mass velocities ($G_T < 500$ kg/m^2 s), and is judged by Whalley[29] to yield reasonable results.

Taitel-Dukler

Taitel and Dukler[25] developed a mathematical model for liquid holdup and pressure drop for horizontal stratified flow, which is illustrated schematically in Fig. 3. A momentum balance on each of the phases yields

$$\text{liquid:}\quad A_l(dp/dz)_{2\Phi} - \tau_{wl}\overline{P}_l + \tau_i S_i = 0 \tag{17}$$

$$\text{gas:}\quad A_g(dp/dz)_{2\Phi} - \tau_{wg}\overline{P}_g + \tau_i S_i = 0 \tag{18}$$

where τ = shear stress; $\overline{P}$ = perimeter over which stress acts; S = interfacial width; and A = cross-sectional area.

$$\tau_{wl} = f_l(\rho_l u_l^2/2) \tag{19}$$

$$\tau_{wg} = f_g(\rho_g u_g^2/2) \tag{20}$$

$$\tau_i = f_i(\rho_g u_g^2/2) \tag{21}$$

where f is the single-phase Blasius friction factor and u is the actual flow velocity. Taitel and Dukler make the assumption that $f_i = f_g$.

By eliminating the pressure gradient between Eq. (17) and (18), the following equation results:

$$\tau_{wg}\frac{\overline{P}_g}{A_g} - \tau_{wl}\frac{\overline{P}_l}{A_l} + \tau_i\left(\frac{S_i}{A_l} + \frac{S_i}{A_g}\right) = 0 \tag{22}$$

From Eq. (22), it is possible to obtain the void fraction as a function of the Lockhart-Martinelli parameter, X, alone. This is equivalent to determining the depth of the stratified liquid layer, h, or in dimensionless from h/D. Similarly, the pressure drop multiplier Φ_g^2 can be obtained from Eq. (18) as a function of X alone.

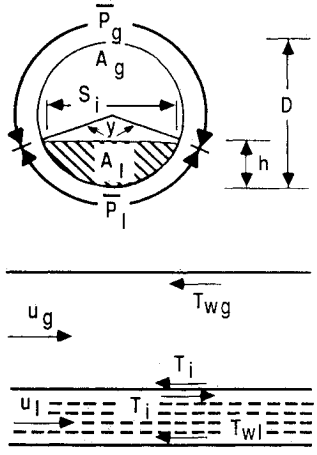

Fig. 3 Two-phase horizontal stratified flow system.

Chisholm Stratified Model

For stratified flow in horizontal tubes, Chisholm[26] compared the Lockhart-Martinelli expression for the pressure drop multiplier, Φ_g^2, with experimental results. From this comparison he recommended that the coefficient C in Eq. (9) should have a value of 1.5, yielding the expression:

$$\Phi_g^2 = 1 + 1.5X + X^2 \tag{23}$$

Annular Flow Model

For the reduced-gravity fight tests at vapor qualities greater than 15%, the flow pattern observed was exclusively annular. Consequently, it is appropriate to correlate the reduced-gravity pressure drops to an annular flow model. For the simplified case of an annular flow with no entrainment and a "smooth" interface, Collier[30] shows that

$$\left(\frac{dp}{dz}\right)_{2\Phi} = \frac{4\tau_i}{(D - 2\delta)} \tag{24}$$

where δ is the annular film thickness, and the interfacial shear stress, τ_i, is given as

$$\tau_i = f_i\left|\rho_g\frac{(u_g - u_i)^2}{2}\right| \tag{25}$$

where ρ_g is the gas density, f_i is the interfacial friction factor, u_g is the mean vapor core velocity and u_i is the interfacial velocity. Because $u_g = j_g/\alpha$ and assuming the interfacial velocity is negligible, then

$$\tau_i = f_i\left|\rho_g\frac{(j_g/\alpha)^2}{2}\right| \tag{26}$$

where j_g is the superficial gas velocity and α, the void fraction, is equal to

$$\alpha = \left(1 - \frac{2\delta}{D}\right)^2 \tag{27}$$

For this flow pattern, the two-phase multipliers can be obtained as

$$\Phi_g^2 = \frac{f_i}{f_g\alpha^{2.5}} \tag{28}$$

$$\Phi_l^2 = \frac{1}{(1-\alpha)^2} \tag{29}$$

If the two-phase pressure gradients in Eqs. (28) and (29) are equated, one obtains

$$\frac{\alpha^{2.5}}{(1-\alpha)^2} = \frac{f_i\rho_l}{f_l\rho_g}\left(\frac{x}{1-x}\right)^2 \tag{30}$$

From Eq. (30), two approaches may be taken to calculate pressure drop. One can either provide the void fraction α to calculate the interfacial friction factor, f_i, or provide the interfacial friction factor to calculate void fraction at any given flow conditions. The liquid friction factor, f_l, can be calculated by the Blasius equation. Then substituting α and f_l into Eq. (26) to obtain τ_i, the frictional pressure gradient may be solved from Eq. (24).

For the first approach, the equation for the vapor void fraction can be written as

$$\alpha = \frac{x/\rho_g}{x/\rho_g + \bar{S}(1-x)/\rho_l} \tag{31}$$

where $\bar{S}$ is the slip ratio (vapor velocity/liquid velocity).

For the homogeneous model, $\bar{S} = 1$. However, more accurate predictions of void fraction must take into account the differences in phase velocities that generally exist in two-phase flows.

The Premoli et al.[24] algorithm is based on a correlation for slip ratio that covers a reasonably wide range of data and accounts for mass flux effects. The slip ratio is given by the expression

$$\bar{S} = 1 + E_1\left(\frac{y}{1 + E_{2y}} - E_{2y}\right)^{1/2}$$

where

$$y \equiv \beta/(1 - \beta)$$

$$\beta \equiv j_g/(j_g + j_l)$$

$$E_1 \equiv 1.578\, Re^{-0.19}(\rho_l/\rho_g)^{0.022}$$

$$E_2 \equiv 0.0273\, We\, Re^{-0.51}(\rho_l/\rho_g)^{-0.08}$$

$$Re \equiv GD/\mu_l$$

$$We \equiv G_T^2 D/(\sigma\rho_l) \qquad (32)$$

For the second approach, the possible relationships for interfacial friction factor have been studied extensively. The interfacial friction factor correlations proposed by Wallis,[31] Henstock and Hanratty,[32] and Asali and Hanratty[33] have been used in this study to solve α from Eq. (30). The pressure drop predicted by the foregoing friction factor models consistently exceeded the data by 100–200% at all qualities.

Using the limited data from the flight experiment, an attempt has been made to empirically extract interfacial friction factor. Based on the high-quality reduced the gravity data, this empirical correlation is

$$f_i = f_g\left|1 + 11.7\left(\frac{\delta}{D}\right)^{0.039}\right| \qquad (33)$$

The same form of the equation, but with a different coefficient and power dependence for the (δ/D) term, have been used by Moeck,[34] Bharathan,[35] and Subbotin et al.,[36] for annular flow models. These correlations are based primarily on air-water flows in small pipes.

In the present study, film thickness was not measured. However, for the relation shown in Eq. (33), an iteration process was used to solve for the interfacial friction factor from Eq. (30) by converging the void fraction. The iteration process is repeated until the calculated pressure drop and the measured data differ by a small tolerance. Only the annular flow data, with qualities above 0.15, were used to formulate Eq. (33).

Therefore, using Eq. (33) for f_i should be expected to produce good agreement with the measured pressure drops in situations where the flow pattern is predominately annular. For cases where the flow pattern is predominately bubbly or slug flow, i.e., for qualities less than 15% in the flight test, Beattie and Whalley's homogeneous model[23] would be appropriate.

Results and Discussion

Figure 4 compares several pressure drop predictions for the average mass flux of 213 kg/m²-s (43.5 lbm/ft²-s) with ground pressure drop data for which flow rates vary from 122 to 308 kg/m²-s (25 to 63 lbm/ft²-s). The curves of Lockhart-Martinelli,[19] Troniewski and Ulbrich,[20] Chisholm B.,[22] and Friedel[21] are seen to lie considerably higher than the measured ground pressure drops. The Beattie and Whalley curve[23] also slightly overpredicts the data. Only the stratified models of Taitel and Dukler[25] and Chisholm[26] result in good agreement with the experimental data, because the flow patterns observed in the ground tests were predominately stratified and semiannular.

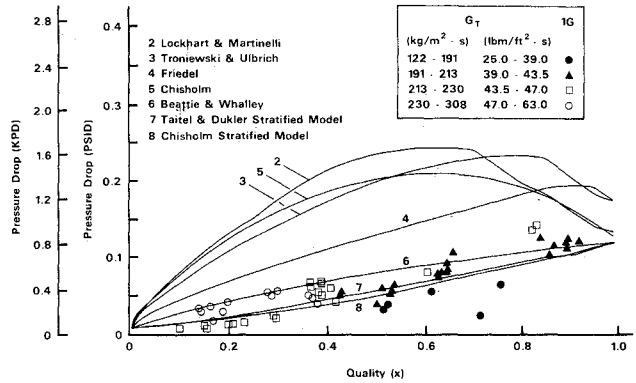

Fig. 4 Comparison between ground test data and seven predictions for a total mass flow rate of 213 kg/m² s at 65.6°C (43.5 lbm/ft² s at 150°F).

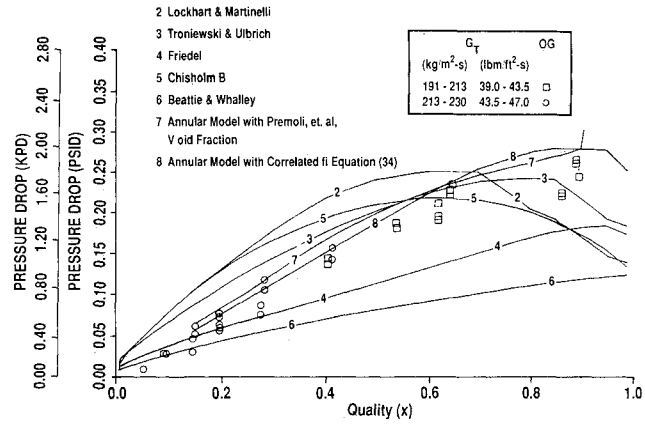

Fig. 5 Comparison between reduced-gravity data and seven predictions for a total mass flow rate of 213 kg/m² s at 63.9°C (43.5 lbm/ft² s at 147°F).

Figure 5 shows the comparison of nine predictions with the reduced-gravity pressure drop measurements. Care should be taken in interpreting this figure because the curves were generated using an average mass flux, whereas the actual mass fluxes varied over a small range 190–230 kg/m²-s or (39 ~ 47 lbm/ft²-s). The curves of Lockhart and Martinelli,[19] Troniewski and Ulbrich[20] and Chisholm[22] overpredict the low quality ($x < 0.6$) data and underpredict at high qualities. In the region where a Taylor bubble slug flow pattern was observed to exist ($x < 0.15$), the Beattie and Whalley homogeneous model[23] correlates well. At qualities higher than 15%, however, the model is not valid due to the occurrence of annular flow. The Friedel method is gravity-dependent, but incorrectly predicts that pressure drops in reduced gravity are less than pressure drops in 1 G, based on the actual pressure drop measurements made in the present experimental study. Typically, the design point of a mixed two-phase thermal management system is at the highest pressure drop condition, normally at high quality. One would be well advised not to use this correlation for the design point sizing of space application systems because it is not conservative at the high-quality condition.

Two annular flow models have been developed in the present study for use in predicting pressure drops in a low-gravity environment. The first of these uses Premoli's void fraction correlation,[24] while the second fits an empirically based interfacial friction factor, Eq. (33). Both models showed good agreement with the reduced-gravity data. At very high-vapor qualities, the void fraction of the Premoli algorithm approaches unity with increasing quality. Equation (30) shows that as the void fraction becomes unity the interfacial friction

Table 4 Summary of pressure drop predictions for reduced and ground gravity tests

	Reduced-gravity test		Ground test	
	Average error*	Standard deviation	Average error	Standard deviation
Lockhart and Martinelli (19)	0.833	1.128	3.525	2.679
Troniewski and Ulbrich (20)	0.553	0.963	2.838	2.063
Friedel (21)	−0.104	0.544	1.606	1.265
Chisholm B (22)	0.748	1.139	3.294	2.750
Beattie and Whalley (23)	−0.344	0.403	0.600	0.804
Annular Flow Model with Premoli's Void Fraction (24)	0.121	0.349	—	—
Taitel and Dukler's Stratified Flow Model (25)	—	—	0.021	0.339
Chisholm's Stratified Flow Correlation (26)	—	—	−0.062	0.296
Annular Flow Model with Correlated Interfacial Friction Factor Equation (33)	0.090	0.320	—	—

*Average error $= \left(\frac{DP_{pred} - DP_{test}}{DP_{test}}\right)_{avg}$.

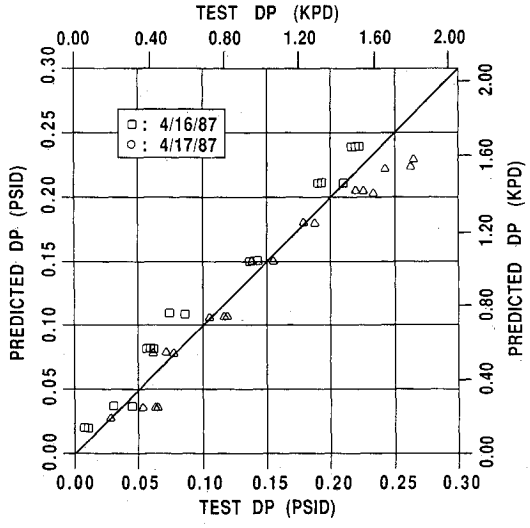

Fig. 6 Comparison of reduced-gravity data to predictions of an annular flow model, Eq. (33).

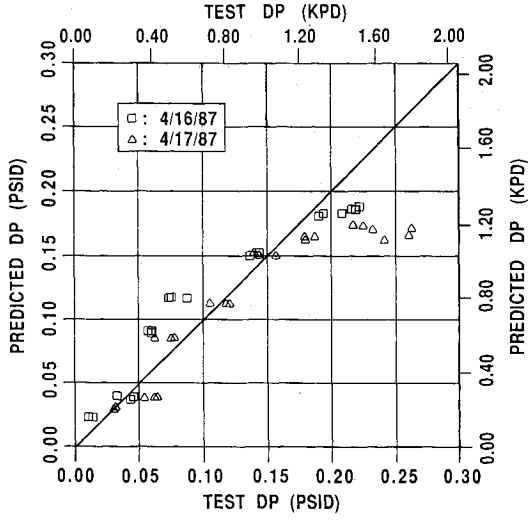

Fig. 7 Comparison of reduced-gravity data to predictions of annular flow model using the Premoli void fraction factor.

factor becomes unbounded. This is unrealistic in that at extremely high qualities, the flow regime will no longer be annular but should be a mist flow. As previously noted, however, the existence of mist flow was not observed at the highest qualities. This indicates that the upper limit of applicability

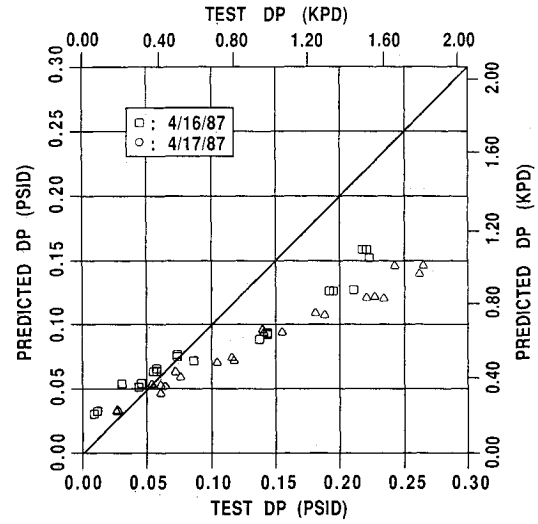

Fig. 8 Comparison of reduced-gravity data to predictions of the Friedel model.

of the annular flow models developed here must be established by testing at higher qualities (and also a wide range of mass fluxes). By testing a variety of fluids over a suitable range of tube sizes, a more universal correlation for this threshold point can be determined. Also, additional reduced gravity tests from which the film thickness and interfacial friction factor could be obtained would be useful in improving the annular flow model.

A statistical comparison of the prediction techniques is given in Table 4, showing the sample error and standard deviation for each. For the ground test data, the Chisholm[26] and Taitel-Dukler's[25] stratified models are seen to correlate best with the data. The Taitel-Dukler model is empirically obtained. For the reduced-gravity data, by contrast, two annular flow models best match the data.

Figures 6–8 compared the reduced-gravity test data to three algorithms. Figures 6 and 7 show that the two annular flow models correlate the data quite well, except at the highest pressure drop levels (for $x < 0.8$), where the annular flow model using Premoli's void fraction underpredicts the test data significantly. Figure 8 shows that the Friedel model[21] tends to substantially underpredict the data, especially at high-vapor quality.

Conclusions

The following conclusions may be drawn from the comparison made herein of pressure drop correlations from sev-

eral models with measured values of pressure drop for both normal-gravity and low-gravity conditions.

1) For two-phase flow inside tubes, the pressure drop is strongly affected by the flow regimes. Consequently, to most accurately predict pressure drop, the flow regime of the mixture must be known or predictable.

2) Pressure drops occurring in two-phase flow under reduced-gravity conditions are significantly greater than those under 1-G conditions for the same conditions of mass flux and quality.

3) The stratified flow models of Taitel-Dukler,[25] and Chisholm[26] provides the most accurate predictions of the ground pressure drop data.

4) The annular flow models developed herein, agree well with the reduced-gravity pressure drop data. The transition point between mist and annular flow was not observed in the testing. Therefore, the upper limit of the range of applicability of the annular flow model could not be established.

5) The Beattie and Whalley homogeneous model[23] appears to correlate the pressure drop data in the bubble (i.e., large single bubbles as opposed to a dispersion of small bubbles) and slug flow regimes, but in this range of low-vapor quality ($x < 0.15$), uncertainty in measured values of pressure drop is relatively larger.

6) The annular flow models presented here are preliminary in that the data base for microgravity two-phase flow patterns and pressure drop is very limited. As more experimental data is available, these methods can be refined.

Acknowledgments

This work resulted from data generated under contract NAS9-17195 with the NASA Johnson Space Center, with Richard Parish as the Technical Program Monitor.

References

[1]Papell, S., "An Instability Effect for Two-Phase Heat Transfer for Subcooled Water Flowing Under Conditions of Zero Gravity," *Proceedings of American Rocket Society Space Power System Conference*, Santa Monica, CA, September 1962.

[2]Evans, D. G., "Visual Study of Swirling and Nonswirling Two-Phase Two-Component Flow at 1 and 0 Gravity," NASA TM-725, August 1963.

[3]Albers, J. A., and Macosko, R. P., "Experimental Pressure-Drop Investigation of Nonwetting, Condensing Flow of Mercury Vapor in a Constant-Diameter Tube in 1-G and Zero-Gravity Environments," NASA TN D-2838, 1965.

[4]Albers, J. A., and Macosko, R. P., "Condensation Pressure Drop of Nonwetting Mercury in a Uniformly Tapered Tube in 1-G and Zero-Gravity Environments," NASA TN D-3185, 1966.

[5]Block, H. B., Crabs, C. C., Mocosko, R. P., and Namkoong, D., "Photographic Study of Condensing Mercury Flow in 0-G and 1-G Environments," NASA TN D-4023, 1967.

[6]Feldmanis, G. J., "Performance of Boiling and Condensing Equipment Under Simulated Outer Space Conditions," ASD-TDR-63-862, November 1963.

[7]Williams, J. L., Keshock, E. G., and Wiggins, C., "Development of a Direct Condensing Radiator for Use in a Spacecraft Vapor Compression Refrigeration System," *ASME Transactions, Journal of Engineering for Industry*, Vol. 5, No. 4, 1973.

[8]Keshock, E. G., Williams, J. L., Spencer, G., and French, B., "An Experimental Study of Flow Condensation Phenomena Under Zero-Gravity Conditions in a Space Radiator System," *Proceedings of Fifth International Heat Transfer Conference*, Vol. IV, Tokyo, Japan, September 1974, pp. 236–240.

[9]Keshock, E. G., "Experimental and Analytical Investigation of 0-G Condensation in a Mechanical Refrigeration System Application," TR 75-T6, Old Dominion University, Contract NAS9-13410, May 1975.

[10]Hepner, D. B., King, C. D., and Littles, J. W., 1975 Zero-G Experiments in Two-Phase Flow Regimes, ASME Paper 75-ENAS-24.

[11]Dukler, A. E., Fabre, J. A., McQuillen, J. B., and Vernon, R., "Gas Liquid Flow at Microgravity Conditions: Flow Patterns and Their Transitions," *International Journal of Multiphase Flow*, Vol. 14, No. 14, 1988, pp. 389–400.

[12]Hill, D., and Downing, R. S., "A Study of Two-Phase Flow in a Reduced Gravity Environment," Final Report, Sundstrand Energy Systems, Contract NAS9-17195, October 1987.

[13]Hill, D. G., Hsu, K., Parish, R., and Dominick, J., "Reduced Gravity and Ground Testing of a Two-Phase Thermal Management System for Large Spacecraft," *Paper presented at the 18th Intersociety Conference on Environmental System*, SAE Paper 881084, San Francisco, CA, July 11–13, 1988.

[14]Rezkallah, K. S., "Two-Phase Flow and Heat Transfer at Reduced Gravity: A Literature Survey," *ANS Proceedings of the National Heat Transfer Conference*, Houston, TX, 1988.

[15]Abdollahian, D., "Study of Two-Phase Flow and Heat Transfer in Microgravity," Final Phase Report, Contract F29601-87-C-0043, Air Force Weapons Lab, Kirtland AFB, NM, January, 1988.

[16]Siegel, R., "Effects of Reduced Gravity on Heat Transfer," *Adv. in Heat Transfer*, Vol. 4, Academic Press, New York, 1967.

[17]Stark, J. A. et al., "Low G Fluid Behavior Technology Summaries," NASA CR-134746, December 1974.

[18]Chen, I. Y., Downing, R. S., Parish, R., and Keshock, E., "A Reduced Gravity Flight Experiment: Observed Flow Regimes and Pressure Drops of Vapor and Liquid Flow in Adiabatic Piping," *AIChE Symposium Series*, Vol. 84, No. 263, Houston, TX, 1988, pp. 203–216.

[19]Lockhart, R. W., and Martinelli, R. C., "Proposed Correlations of Data for Isothermal Two-Phase Two-Component Flow in Pipes," *Chemical Engineering Program*, Vol. 45, 1949, pp. 39–48.

[20]Troniewski, L., and Ulbrich, R., "Two-Phase Gas-Liquid Flow in Rectangular Channels," *Chemical Engineering Science*, Vol. 39, No. 4, pp. 751–765, 1984.

[21]Friedel, L., "Improved Pressure Drop Correlations for Horizontal and Vertical Two-Phase Pipe Flow," *3R International*, Vol. 18, No. 7, 1979, pp. 485–492.

[22]Chisholm, D., "Pressure Gradients Due to Friction During The Flow of Evaporating Two-Phase Mixtures in Smooth Tubes and Channels," *International Journal of Heat Mass Transfer*, Vol. 16, 1973, pp. 347–358.

[23]Beattie, D. R. H., and Whalley, P. B., "A Simple Two-Phase Frictional Pressure Drop Calculation Method," *International Journal of Multiphase Flow*, Vol. 8, No. 1, 1982, pp. 83–87.

[24]Premoli, A., DiFrancesco, D., and Prina, A., "An Empirical Correlation for Evaluating Two-Phase Mixture Density Under Adiabatic Conditions," European Two-Phase Flow Group Meeting, Milan, Italy, 1970.

[25]Taitel, Y., and Dukler, A. E., "A Theoretical Approach to the Lockhart-Martinelli Correlation for Stratified Flow," *International Journal of Multiphase Flow*, Vol. 2, 1976, pp. 591–595.

[26]Chisholm, D., Two-Phase Flow in Pipelines and Heat Exchangers, George Godwin, London, p. 133, 1983.

[27]Chisholm, D., "A Theoretical Basis for the Lockhart-Martinelli Correlation for Two-Phase Flow," International Journal of Heat and Mass Transfer, Vol. 10, pp. 1767–1778, 1967.

[28]Troniewski, L. and Ulbrich, R., "Two-Phase Gas-Liquid Flow: Author's Reply," *Chemical Engineering Science*, Vol. 40, No. 10, pp. 2000–2002, 1985.

[29]Whalley, P. B., Two-Phase Pressure Drop Design Report, HTFS DR28, Part 5, AERE-R 9793, 1981.

[30]Collier, J. G., Convective Boiling and Condensation, McGraw-Hill Company, page 81, 1981.

[31]Wallis, G. B., One Dimensional Two-Phase Flows, McGraw-Hill Book Company, 1969.

[32]Henstock, W. H. and Hanratty, T. J., "The Interfacial Drag and the Height of the Wall Layer in Annular Flows," *AIChE Journal*, Vol. 22, 1976.

[33]Asali, J. C. and Hanratty, T. J., "Interfacial Drag and Film Height for Vertical Annular Flow," *AIChE Journal*, Vol. 31, No. 6, pp. 895–902, 1985.

[34]Moeck, W. A., "Annular-Dispersed Two-Phase Flow and Critical Heat Flux," PhD. Thesis, McGill Univ., Montreal, Quebec, Canada, 1970.

[35]Bharathan, D., "Air-Water Counter Current Annular Flow," Electric Power Research Institute Report, EPRI NP-1165, 1979.

[36]Subbotin, V. I., Sorokin, D. N., Nigmatulin, B. I., Milashenko, V. I., and Nikolayer, V. E., "Integrated Investigation into Hydrodynamic Characteristics of Annular Dispersed Steam-Liquid Flows," Sixth Int. Heat Transfer Conference, Toronto, Vol. 1, pp. 327–337, 1978.